Regular Article

ANALYTICAL
AND BIOANALYTICAL
CHEMISTRY
RESEARCH

Published by the
Iranian Chemical Society

***Anal. Bioanal. Chem. Res.**, Vol. 11, No. 4, 415-421, September 2024.*

A Sensitive Colorimetric Assay for Acetylcholinesterase Activity based on Aggregation of Gold Nanoparticles with Phosalone

Khatereh Pashangeh[a,b] and Safoora Pashangeh[c,*]

[a]*Department of Food Science and Technology, Tarbiat Modares University, Tehran, Iran*
[b]*Professor Massoumi Laboratory, Department of Chemistry, Shiraz University, Shiraz 71454, Iran*
[c]*Department of Food Science and Technology, Faculty of Agriculture, Jahrom University, Jahrom, Iran*
(Received 21 November 2023, Accepted 20 May 2024)

A highly sensitive, fast, and convenient colorimetric assay for acetylcholinesterase (AChE) activity was developed. To do this, phosalone was used to aggregate citrate-coated gold nanoparticles which caused its color to be changed from wine-red to blue. This aggregation was significantly hindered with AChE, due to its preferential reaction with phosalone, and the corresponding color change was probed spectrophotometrically as a function of AChE activity. The ratio of the measured absorbances at the wavelengths of 520 and 650 nm (A520/A650) was found to be linear with the activity of AChE from 0.050 to 1.0 U ml^{-1} ($R^2 = 0.9912$). A limit of 0.030 U ml^{-1} for detection of AChE was achieved based on a signal-to-noise ratio of 3. The procedure was successfully applied for the determination of AChE in real samples as well as quantitation of phosalone in diverse fields such as food and agricultural industries as well as pharmaceutical, healthcare, and environmental affairs.

Keywords: Acetylcholinesterase, Phosalone, Gold nanoparticles, Aggregation, Colorimetric assay

INTRODUCTION

Acetylcholinesterase (AChE) has been reported to have a fundamental role in nerve-agent poisoning, inflammatory processes, and symptomatic treatment of Alzheimer's disease [1]. This enzyme can be found in body tissues such as red blood cells and the post-synaptic membrane of cholinergic synapses. It can terminate the cholinergic nerve transmission and can inactivate acetylcholine (ACh) by hydrolyzing it to acetate and choline and halt the nerve impulse. Therefore, a reliable and sensitive assay, in order to determine and/or monitor the activity of AChE, is of great concern in multifarious fields. The AChE inhibitors are principal drugs [2] that are able to penetrate the blood-brain barrier. For instance, the hydrolysis of ACh (by AChE) can be prevented by inhibitors such as organophosphate (OP). Due to this, the concentration of ACh in the synaptic cleft is increased which has been frequently considered as a basis for diagnosing organophosphate poisoning [3]. It is worth mentioning that organophosphate (OP) neurotoxins, which are commonly used as insecticides and pesticides as well as warfare agents, are well known to be toxic. Because of this, their usage is of great concern in agricultural and military activities [4-8] as their residue may cause various health difficulties for all the beings in the various ecosystems [9]. The toxicity of these compounds is due to the inactivation and irreversible phosphorylation [10] of AChE in both the peripheral and central nervous system as reported [11-16].

In terms of simplicity and speed, the colorimetric sensors are favorable for the detection of materials such as AChE [17]. In this regard, utilization of plasmonic nanoparticles such as gold [18-20] is promising as they have been widely incorporated for analysis of different organic and inorganic compounds [21-37] due to their high extinction coefficients

*Corresponding author. E-mail: s.pashangeh@jahromu.ac.ir

($\approx 3 \times 1011$ M cm^{-1}).

Biosensor-based detection of neurotoxins offers a promising approach due to its ease of use, speed, cost-effectiveness, portability, specificity, and high sensitivity without requiring lengthy procedures. Electrochemical biosensors for detecting organophosphates (OPs) have been particularly successful due to their simple instrumentation, high reliability, and compatibility with complex samples [38-39]. Enzyme-based biosensors are an excellent alternative for detecting insecticides and pesticides, including OPs, as these toxins inhibit various insect and pest enzymes, including acetylcholinesterase (AChE). Oxidase-mimicking materials such as MnO_2 nanosheets and surface-modified cerium oxide nanoparticles have been utilized to generate signals for OP detection through colorimetry *via* tetramethylbenzidine (TMB) oxidation [40-41]. Previous studies have employed colorimetric detection systems based on TMB, nanozymes, and hydrogen peroxide [42-43].

The term "nanozyme" was first coined to describe gold nanoparticles (AuNPs) possessing transphosphorylation capabilities. Nanozymes are nanomaterials capable of mimicking enzyme functions [44]. These materials are easy to synthesize and exhibit higher stability than proteins under harsh conditions [45], making them highly desirable for applications in environmental monitoring [46-47]. Enzyme-mimicking materials can be categorized into two classes: oxidoreductases and hydrolases [48]. Colorimetric nanoenzyme-based biosensing of OPs is a simple approach that allows for on-site monitoring of these compounds with the naked eye, eliminating the need for readout instruments.

Based on different surface plasmon resonance behavior of gold nanoparticles in aggregation and non-aggregation (dispersion) states, a two-step optical detection system for the determination of AChE was constructed without any modification or enzyme-immobilization processes. Phosalone was used as the aggregation-induced agent which immediately changed the color of AuNPs from red to blue when it was mixed with the nanoparticle solution. In the next step, the color of this solution was retained when AChE was added. The changes in the magnitude of the AuNPs absorbance, as will be described later, were probed as a function of AChE concentration which was the basis for its quantification.

EXPERIMENTAL

Materials

Acetylcholinesterase (AChE) from Drosophila Melanogaster (1500 IU/ml) was provided by TAHABIOTECH Corporation (Tehran, Iran) and stored at -18 °C. Phosalone and acetylcholine iodide (ATC) were purchased from Sigma-Aldrich Corporation. The DTNB (5-5′-dithiobis-(2-nitrobenzoic acid) was supplied by Wako Pure Chemical Industries (www.wako-chem.co.jp). $HAuCl_4.3H_2O$, with a 99.5% purity was provided from Merck. Other chemicals were of analytical grades. For the preparation of aqueous solutions and in all the experiments, Milli-Q grade water (18.2 MΩ) was employed.

Instrumentation

A Lambda spectrophotometer (PerkinElmer, USA), equipped with a glass cell (1.0 cm), was employed for measuring the absorbance values. A Denver (Model 270) pH meter with a Metrohm glass electrode was utilized for measuring the values of the pH of the aqueous solutions. For recording the TEM images, a PHILIPS MC 10 TH microscope, working at an accelerating voltage of 100 kV, was employed. A Malvern Zetasizer Viscotek 802, working at ambient temperature, was utilized for specifying the particle size and patterns of the synthesized nanoparticles.

Synthesis of Gold Nanoparticles

Citrate-coated AuNPs were prepared based on the modified Turkevich procedure [49-50]. To do this, 50 ml of 1.0 mM $HAuCl_4$ aqueous solution was heated, while stirring, up to its boiling point. To this solution, a volume of 5.0 ml of 38.8 mM sodium citrate was added gradually to achieve a change in color (yellow to wine red) representing that old nanoparticles were produced. After refluxing and stirring for 30 min, followed by cooling to room temperature, the AuNPs sample was kept in the dark at 4.0 °C.

AChE Activity Assay

The activity of AChE hydrolytic was determined with ATC (acetylcholine iodide) as the substrate [51]. The working solutions were made of 40 µl of the enzyme solution, 40 µl of 1.5 mM ATC, and 20 µl of 0.30 mM DTNB, mixed in 140 µl of 0.10 M buffer (phosphate buffer with pH 7.0).

After incubating at 37 °C for 30 min, the absorbance of the enzyme was determined in 5-minute intervals at 405 nm followed by calculating its activity [52].

RESULTS AND DISCUSSION

The pesticide phosalone (Scheme 1) has a great affinity, due to its thiol functional group, for interacting with AuNPs if appropriate functioning groups are available at their surface.

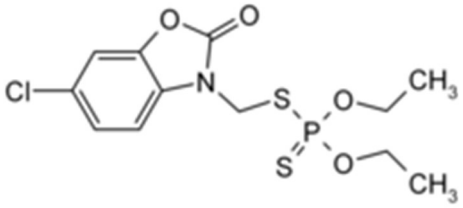

Scheme 1. Phosalone molecular structure

Therefore, it is expected to be able to aggregate citrate-coated gold nanoparticles through developing some interactions namely H-bonding and/or electrostatic interactions. However, the SPR (surface plasmon resonance) band of AuNPs decreases when phosalone is present and a new SPR band arises due to the re-dispersion of AuNPs. These aggregation/dispersion processes for AuNPs were probed spectrophotometrically in the UV-Vis range of the electromagnetic radiation (Fig. 1) as well as DLS (dynamic light scattering) and TEM (transmission electron microscopy). It should be mentioned that the dispersion of AuNPs (a ruby red solution) stabilizes in an aqueous solution as electrostatic repulsions develop among the negatively charged capping agents positioned on their surfaces [53]. At the wavelength of 520 nm, an SPR band was observed for AuNPs as shown in Fig. 1. However, a new band was observed at about 650 nm when a certain concentration of phosalone was added. Due to the specifically strong interaction between the thiol groups in phosalone and the gold atoms in AuNPs, phosalone can significantly induce aggregation of gold nanoparticles and cause their color to change from red to blue. By introducing AChE in the system, however, the aggregation of the gold nanoparticles is hindered as phosalone preferentially reacts with AChE. This causes the color of the system to be reverted from blue to red as the nanoparticles disperse again. The hindering action of AChE in the aggregation of AuNPs has been demonstrated through the TEM images and DLS analysis as, respectively, presented in Figs. 2 and 3. To enhance the sensing results, the optimum values of the significant experimental parameters including AuNPs concentration, concentration of phosalone as well as both incubation time and incubation temperature were optimized as discussed below.

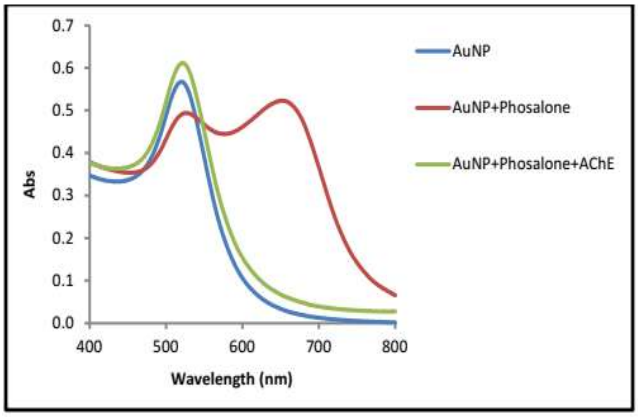

Fig. 1. The UV-Vis Spectrum of as-prepared AuNPs.

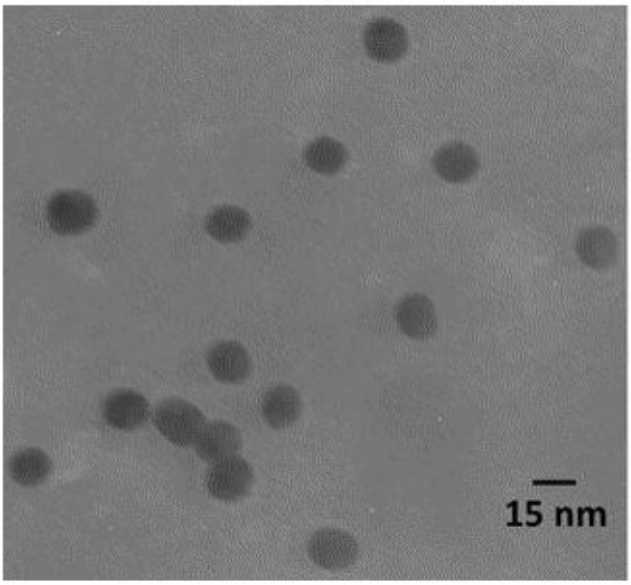

Fig. 2. The TEM images of as-prepared AuNPs.

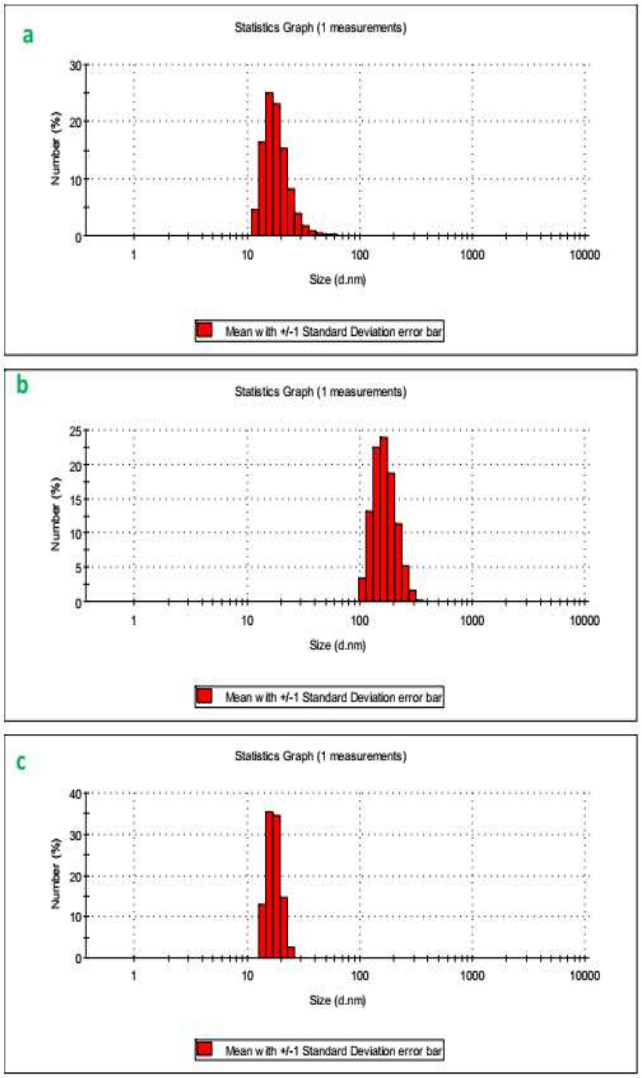

Fig. 3. Size distribution (DLS) of AuNPs a) in the absence of phosalone, b) in the presence of 0.5 mg l^{-1} of phosalone, and c) in the presence of phosalone and 1 unit of AChE activity after 20 min.

AuNP Concentration

Controlling the concentration of AuNPs is another critical parameter that should be taken into consideration to improve the sensitivity of the method. The dispersion of AuNP, under the influence of its concentration in the range of 1.0-4.0 nM, was investigated in the presence of 0.5 mg l^{-1} phosalone. As shown in Fig. 4, the signal (A_{520}/A_{650}) increased up to a concentration of 3.0 nM AuNPs and eventually remained

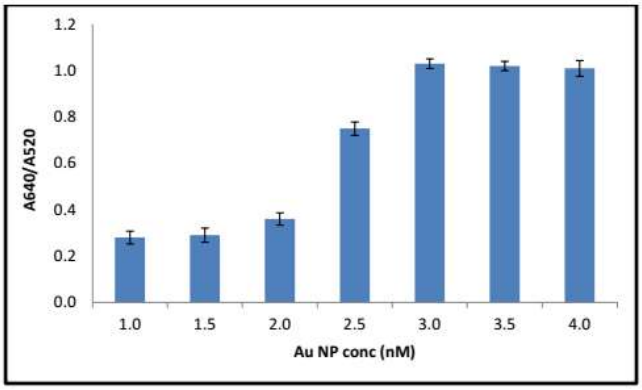

Fig. 4. Effect of Different AuNP concentrations (1.0-4.0 nM) for the aggregation by phosalone. Conditions: 0.5 mg l^{-1} phosalone in 0.1 M phosphate buffer pH = 7.0, 20 min time reaction.

constant. This indicated that aggregation of the AuNPs was completed at 3.0 nM which was then considered as its optimum concentration for continuing the subsequent optimization processes.

Phosalone Concentration

Since the sensitivity of the developed method is under the influence of phosalone, the dispersion of AuNPs in the presence of AChE was studied by probing the signal value (A_{520}/A_{650}) in different phosalone concentrations (Fig. 5). At concentrations more than 0.50 mg l^{-1}, phosalone did not show any significant effect on aggregation of AuNPs. This indicated that a concentration of 0.50 mg l^{-1} phosalone was the least concentration of phosalone required to be present in the reaction system to disclose the blue AuNPs and to achieve a good sensitivity as well as a broader linear dynamic range for the method.

Incubation Temperature and Time

Figure 6 shows the effect of temperature on the activity of AChE by probing the dispersion of AuNPs at different incubating temperatures in the range of 15-40 °C.

For doing this optimization, phosalone and AChE mixed solution, in the phosphate buffer (pH = 7.0), was incubated for 20 min at different temperatures followed by adding AuNPs in order to examine the aggregation of these nanoparticles. Based on the observed results, the temperature

of 25 °C was selected as the optimum value at which minimum aggregation of AuNPs and maximum catalytic activity of AChE was achieved, *i.e.*, a high amount of phosalone molecules reacted with AuNPs. To determine the optimum incubation time, various incubation times were tested. Dispersion of AuNPs by AChE was completely achieved after 25 min of incubating AChE with phosalone as indicated by the obtained results (Fig. 7).

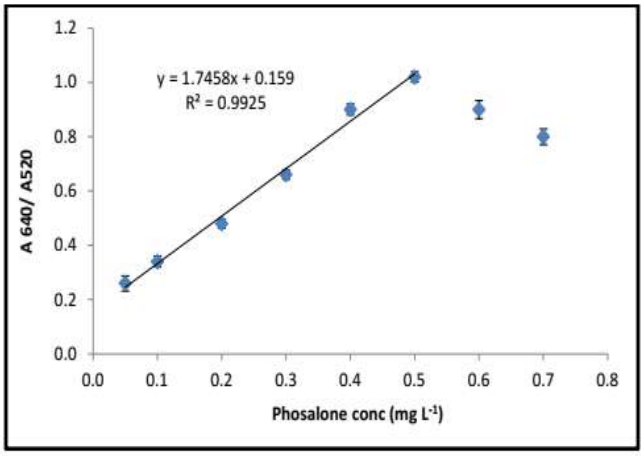

Fig. 5. Linear range of phosalone concentration for the aggregation of AuNPs. Conditions: 3.0 nM of AuNPs in 0.1 M phosphate buffer pH = 7.0, 20 min time reaction.

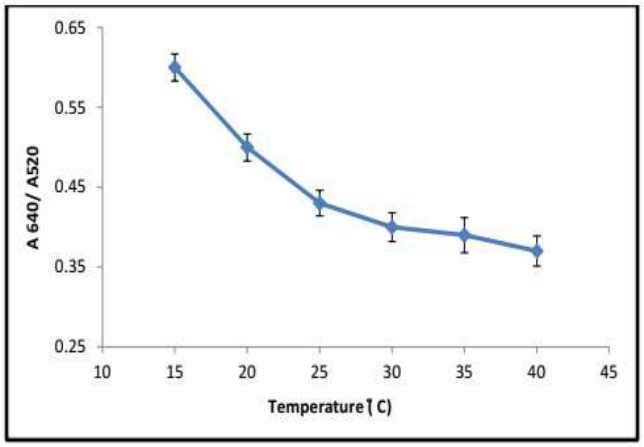

Fig. 6. Effect of incubation temperature on AChE activity for the anti-aggregation of AuNPs with phosalone. Conditions: 3.0 nM of AuNP, 0.5 mg l^{-1} phosalone, 1U of AChE activity in phosphate buffer pH = 7.0, 20 min incubation time.

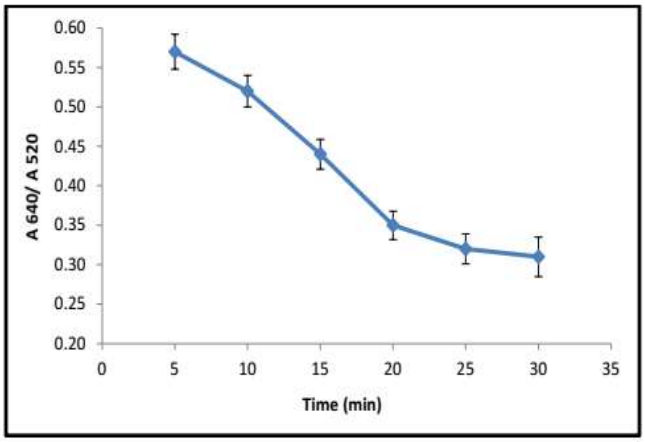

Fig. 7. Effect of incubation time on AChE activity for AuNPs for the anti-aggregation of AuNPs with phosalone. Conditions: 3.0 nM of AuNP, 0.5 mg l^{-1} phosalone, 1U of AChE activity in phosphate buffer pH = 7.0, incubation temperature at 25 °C.

Figures of Merit

After optimizing effective experimental conditions, further experiments revealed that the analytical signal (A_{520}/A_{650}) may directly be related to the quantity of AChE activity as was expected. Figure 8A indicates that by increasing AChE activity, the signal decreased at 650 nm due to aggregation of AuNPs. At 520 nm, an increase in the corresponding signal was observed which was due to the re-dispersion of AuNPs. As shown, in Fig. 8B, the A_{520}/A_{650} ratio increased linearly over the AChE activity in the 0.050-1.0 U ml^{-1}. Because the dynamic range of the probe depended on the concentration of phosalone, the linear range of the AChE activity assay was extended by increasing the phosalone concentration. The detection limit for the probe was determined as 0.030 U ml^{-1} AChE. For evaluating the precision of the technique, the experiments were done three times independently and relative standard deviations of 2.1% for 0.5 mg l^{-1} phosalone and 5.7% for different activities of AChE were achieved.

CONCLUSION

A successful sensitive and simple colorimetric assay for AChE, based on aggregation of AuNPs with phosalone (producing a blue solution) followed by its re-dispersion in

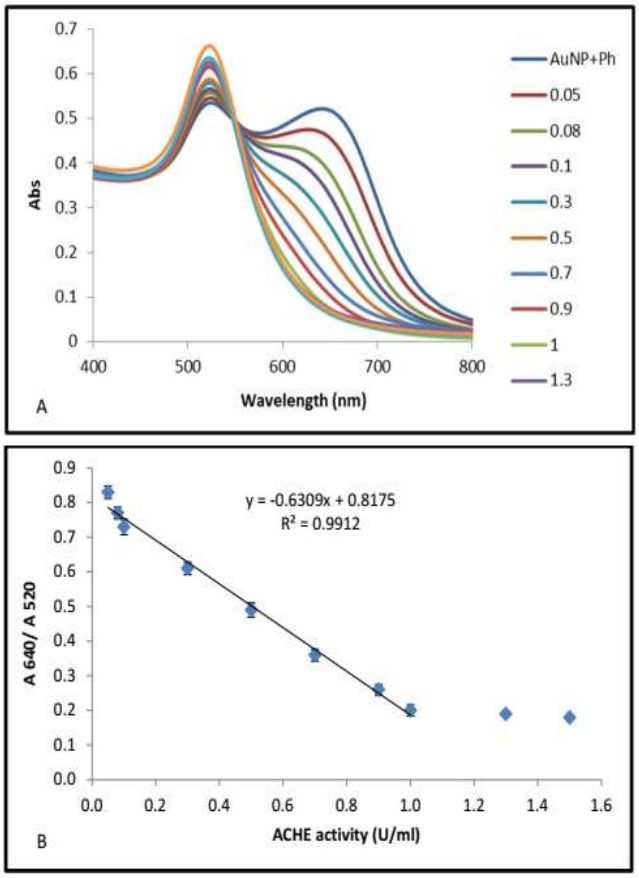

Fig. 8. (A) Surface plasmon resonance band for the anti-aggregation of AuNPs with phosalone in the presence of different AChE activity. (B) Calibration curve of different AChE activity, 0.05-1.5 U ml^{-1} for the anti-aggregation of AuNPs with phosalone. Conditions: 3.0 nM of AuNP, 0.5 mg l^{-1} phosalone, 1U of AChE activity in phosphate buffer pH = 7.0, incubation temperature at 25 °C, incubation time 25 min.

the presence of AChE (producing a red solution), was developed. This assay relies on the distance-dependent surface plasmon resonance band of gold nanoparticles. When thiol-containing phosalone replaces citrate on the surface of the gold nanoparticles, a new peak appears at a longer wavelength, which intensifies and shifts further to the red from the original peak position due to the aggregation of gold nanoparticles. This aggregation depends on the ionic strength, gold nanoparticle concentration, and phosalone concentration. During this process, the plasmon band at 520 nm gradually decreases while a new red-shifted band forms at 650 nm. The several advantages observed for the procedure, made it promising for rapid sensing of AChE in real samples. The response of the probe was linear over the activity of AChE in the range of 0.050-1.0 U ml^{-1} and the detection limit was 0.030 U ml^{-1}. The precision of the technique, in terms of relative standard deviations, was found to be 5.7% for different activities of AChE.

ACKNOWLEDGMENT

All authors of this paper appreciatively acknowledge the Research Councils of Shiraz University (Shiraz, Iran) for financially supporting this reported research.

REFERENCES

[1] J.S. Coggan, T.M. Bartol, E. Esquenazi, J.R. Stiles, S. Lamont, M.E. Martone, D.K. Berg, M.H. Ellisman, T.J. Sejnowski, Science 309 (2005) 446.
[2] H. Dvir, I. Silman, M. Harel, T.L. Rosenberry, J.L. Sussman, Chem. Biol. Interact. 187 (2010) 10.
[3] M. Bajda, A. Więckowska, M. Hebda, N. Guzior, C.A. Sotriffer, B. Malawska, Curr. Med. Chem. 14 (2007) 2654.
[4] W.E. Westlake, Anal. Chem. 35 (1963) 105.
[5] R. Bala, R.K. Sharma, N. Wangoo, Anal. Bioanal. Chem. 408 (2015) 333.
[6] D. Noort, H.P. Benschop, R.M. Black, Toxicol. Appl. Pharmacol. 184 (2002) 116.
[7] B.J. Sanghavi, G. Hirsch, S.P. Karna, A.K. Srivastava, Anal. Chim. Acta 735 (2012) 37.
[8] G.H. Yao, R.P. Liang, C.F. Huang, Y. Wang, J.D. Qiu, Anal. Chem. 85 (2013) 11944.
[9] J. Sun, L. Guo, Y. Bao, J. Xie, Biosens. Bioelectron. 28 (2011) 152.
[10] N. Fahimi-Kashani, M.R. Hormozi-Nezhad, Anal. Chem. 16 (2016) 8099.
[11] S. Nouanthavong, D. Nacapricha, C.S. Henry, Y. Sameenoi, Anlst. 141 (2016) 1837.
[12] C. Dwivedi, A. Gupta, A. Chaudhary, C.K. Nandi, RSC. Adv. 4 (2014) 39830.
[13] G. Xue, Z. Yue, Z. Bing, T. Yiwei, L. Xiuying, L. Jianrong, Anlst. 141 (2016) 1105.

[14] D.M. Quinn, Chem. Rev. 87 (1987) 955.
[15] F. Worek, H. Thiermann, L. Szinicz, P. Eyer, Biochem. Pharmacol. 68 (2004) 2237.
[16] O. Lockridge, L.M. Schopfer, P. Masson, Chapter 56 in Handbook of Toxicology of Chemical Warfare Agents, Gupta, RC, Ed, Academic Press, 2009.
[17] T. Lou, L. Chen, Z. Chen, Y. Wang, J. Li, ACS. Appl. Mater. Interfaces. 3 (2011) 4215.
[18] M.R. Hormozi-Nezhad, J. Tashkhourian, J. Khodaveisic, M.R. Khoshi, Anal. Methods. 2 (2010) 1263.
[19] N.T.K. Thanh, Z. Rosenzweig, Anal. Chem. 74 (2002) 1624.
[20] D. Vilela, M. Cristina Gonzalez, A. Escarpa, Anal. Chim. Acta 751 (2012) 24.
[21] S. Kim, J. Won Park, D. Kim, I. Lee, S. Jon, Chem. Int. Ed. 48 (2009) 4138.
[22] F. Chai, C.H. Wang, T. Wang, L. Li, Z. Su, Interfaces. 2 (2010) 1466.
[23] Y.Q. Dang, H.W. Li, B. Wang, L. Li, Y. Wu, ACS. Appl. Mater. Interfaces. 1 (2009) 1533.
[24] D. Liu, W. Qu, W. Chen, W. Zhang, Z. Wang, X. Jiang, Anal. Chem. 82 (2010) 9606.
[25] Y. Ma, L. Jiang, Y. Mei, R. Song, D. Tian, H. Huang, Anlst. 138 (2013) 5338.
[26] Y. We Gooding, J. Justin He, J. Zhicong, Q. Li, G. Chen, Nanosci. Nanotechnol. 7 (2007) 712.
[27] J. Du, B. Zhu, X. Chen, Small. 9 (2013) 4104.
[28] W.L. Daniel, M.S. Han, J.S. Lee, C.A. Mirkin, J. Am. Chem. Soc. 131 (2009) 6362.
[29] Y. Zhou, Z. Yang, M. Xu, Anal. Methods. 4 (2012) 2711.
[30] W. Pu, H. Zhao, C. Huang, L. Wu, Anal. Chim. Acta 764 (2013) 78.
[31] X. Wang, O. Ramstrom, M.D. Yan, Anal. Chem. 82 (2010) 9082.
[32] C.L. Schofield, B. Mukhopadhyay, S.M. Hardy, M.B. McDonnell, R.A. Field, D.A. Russell, Anlst. 133 (2008) 626.
[33] H.M. Zakaria, A. Shah, M. Konieczny, J.A. Hoffmann, A. Jasper Nijdam, M.E. Reeves, Langmuir. 29 (2013) 7661.
[34] N. Uehara, K. Ookubo, T. Shimizu, Langmuir. 26 (2010) 6818.
[35] S.C.B. Gopinath, T.H. Tang, S. Yi, M. Citartan, Biosens. Bioelectron. 64 (2015) 392.
[36] P. Liu, X. Yang, S.H. Sun, Q. Wang, K. Wang, J. Huang, J. Liu, L. He, Anal. Chem. 85 (2013) 7689.
[37] C.D. Medley, J.E. Smith, Z.H. Tang, Y. Wu, S. Bamrungsap, W. Tan, Anal. Chem. 80 (2008) 1067.
[38] B. Wang, Y. Li, H. Hu, W. Shu, L. Yang, J. Zhang, PLoS ONE. 15 (2020) e0231981.
[39] H. Hu, L. Yang, J. Environ. Sci. Health Part B. 56 (2020) 168.
[40] X. Yan, Y. Song, X. Wu, C. Zhu, X. Su, D. Du, Y. Lin, Nanoscale 9 (2017) 2317.
[41] S.-X. Zhang, S.-F. Xue, J. Deng, M. Zhang, G. Shi, T. Zhou, Biosens. Bioelectron. 85 (2016) 457.
[42] T. Jiang, Y. Song, T. Wei, H. Li, D. Du, M.-J. Zhu, Y. Lin, Biosens. Bioelectron. 77 (2016) 687.
[43] W. Ren, W. Liu, J. Irudayaraj, Sens. Actuators B Chem. 247 (2017) 923.
[44] Y. Wu, D.C. Darland, J.X. Zhao, Sensors 21 (2021) 5201.
[45] Q. Wang, H. Wei, Z. Zhang, E. Wang, S. Dong, TrAC Trends Anal. Chem. 105 (2018) 218.
[46] P.G. Arias, H. Martinez-Perez-Cejuela, A. Combes, V. Pichon, E. Pereira, J.M. Herrero-Martinez, M. Bravo, J. Chromatogr. A. 1626 (2020) 461346.
[47] I.-H. Cho, A. Bhunia, J. Irudayaraj, Int. J. Food Microbiol. 206 (2015) 60.
[48] Y. Huang, J. Ren, X. Qu, Chem. Rev. 119 (2019) 4357.
[49] J. Kimling, M. Maier, B. Okenve, V. Kotaidis, H. Ballot, A. Plech, J. Phys. Chem. B 110 (2006) 15700.
[50] J. Liu, Y. Lu, Nat. Protoc. 1 (2006) 246.
[51] G.L. Ellman, K.D. Courtney, V.J. Andres, R.M. Featherstone, Biochem. Pharmacol. 7 (1961) 88.
[52] D.Q. Yin, H.J. Jin, H.X. Yu, L.Y. Chen, Chin. J. Appl. Entomol. 12 (2001) 615.
[53] K.C. Grabar, R.G. Freeman, M.B. Hommer, M.J. Natan, Anal. Chem. 67 (1995) 735.